

Development and Proof of Concept for a Large-Scale Photoredox Additive-Free Minisci Reaction

Mark A. Graham,* Gary Noonan,* Janette H. Cherryman, James J. Douglas, Miguel Gonzalez, Lucinda V. Jackson, Kevin Leslie, Zhi-qing Liu, David McKinney, Rachel H. Munday, Chris D. Parsons, David T. E. Whittaker, En-xuan Zhang, and Jun-wang Zhang



Cite This: <https://dx.doi.org/10.1021/acs.oprd.0c00483>



Read Online

ACCESS |



Metrics & More



Article Recommendations



Supporting Information

ABSTRACT: New route development activities toward ceralasertib (AZD6738) have resulted in the discovery of an efficient, acid additive-free, photoredox Minisci reaction. Mechanistic understanding resulting from LED-NMR reaction profiling, quantum yield measurements, and Stern–Volmer quenching studies have enabled optimization of the catalyst system, resulting in a significant enhancement in the rate of reaction. A large-scale continuous photoflow process has been developed, providing encouraging proof-of-concept data for the future application of this technology in the clinical manufacture of ceralasertib.

KEYWORDS: *Minisci, photoredox, photoflow, ceralasertib, AZD6738, LED-NMR*

INTRODUCTION

Ceralasertib (AZD6738, **1**)^{1–3} is currently being evaluated in multiple phase I/II clinical trials for the treatment of cancer.⁴ Its structure, comprising a pyrimidine core decorated with a chiral morpholine, a cyclopropyl sulfoximine, and an azaindole, makes it a challenging molecule to synthesize on a large scale. The incorporation of the thiomethylcyclopropyl moiety on the pyrimidine ring is especially challenging from a synthesis perspective. A significant improvement in the large-scale synthesis of **1** came with the recently disclosed development of a scalable approach to the thiomethylcyclopropyl acid **2**, shown in Scheme 1.^{5,6} However, in an attempt to further improve the route, we considered the desirable “shortcut” shown in Scheme 1, which would allow for more efficient access to the dichloropyrimidine intermediate **3**.

The classical Minisci reaction⁷ involves the addition of a nucleophilic alkyl radical to a heteroaromatic compound. Typical reaction conditions employ an oxidant, most often a persulfate salt, to induce decarboxylation to an alkyl radical, as well as a Brønsted or Lewis acidic reagent, which is thought to be important to increase the electrophilicity of the heteroarene.⁸ Mai and co-workers recently reported a silver-catalyzed Minisci-type alkylation of 2-chloropyridine using potassium persulfate,⁹ while Shore reported Minisci allylations using a variety of electron-deficient pyrimidines.¹⁰ We hoped that similar conditions would be applicable to our system while being acutely aware of the relatively facile oxidation of sulfur in thioethers. Encouragingly, we were able to demonstrate the conversion of acid **2** to pyrimidine **3** using classical Minisci conditions (Scheme 2), albeit with the accompanying formation of the sulfur oxidation products.

Visible light photocatalytic reactions have exploded in popularity over the past decade, and with this increased interest, a large number of classical radical chemistries have been realized under irradiative conditions.^{11–15} Recent

advances in the scale-up of photochemical processes using continuous flow chemistry were also encouraging when considering light-driven manufacturing processes for a drug substance.^{16–20} We were particularly interested in exploring the approach of Fu,²¹ Sherwood,^{22,23} and Opatz²⁴ who have recently reported effective Minisci reactions using redox active esters under visible light photocatalysis conditions. Crucially, these reactions are redox-neutral; thus, we were optimistic that this chemistry would be compatible with our substrate. Herein, we describe the development work carried out to realize this transformation, as well as the mechanistic and practical insights gleaned from the work. We then demonstrate the proof-of-concept scale-up of this reaction using a photoflow reactor, confirming our process as a viable option for the future manufacture of an active pharmaceutical ingredient (API).

RESULTS AND DISCUSSION

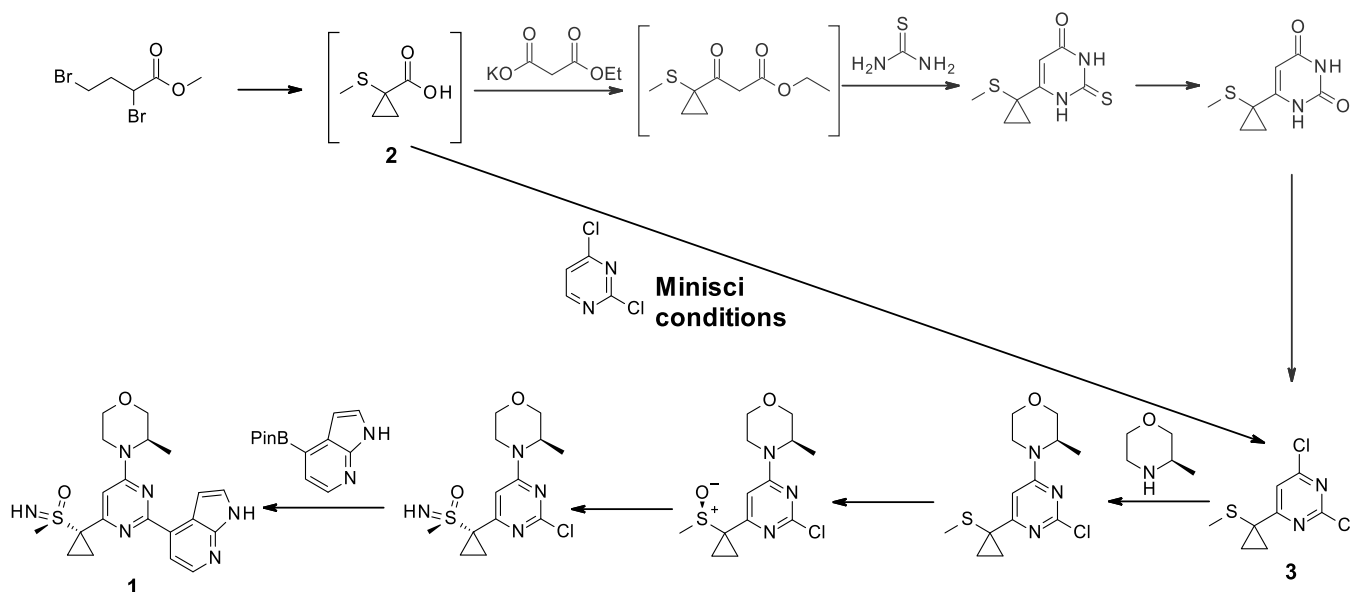
Development of Photoredox Minisci Conditions.

Initially, we investigated the visible-light photoredox reaction under batch conditions, as reported by Sherwood.²² This involved the *in situ* generation of the *N*-hydroxyphthalimide redox active ester **6**, followed by the addition of camphorsulfonic acid and catalytic 1,2,3,5-tetrakis(carbazol-9-yl)-4,6-dicyanobenzene (4CzIPN) in DMSO and irradiation in an EvoluChem photochemical reactor. Pleasingly, the desired product **3** was formed, albeit in a modest isolated yield of 25%, despite full consumption of active ester **6** (Scheme 3).²⁵

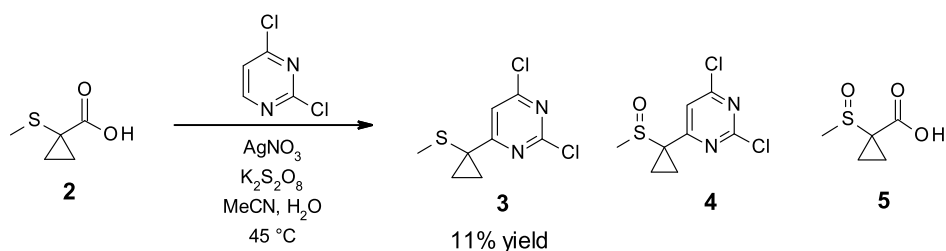
Received: October 27, 2020



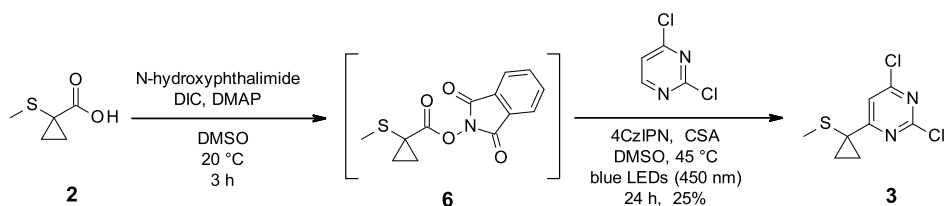
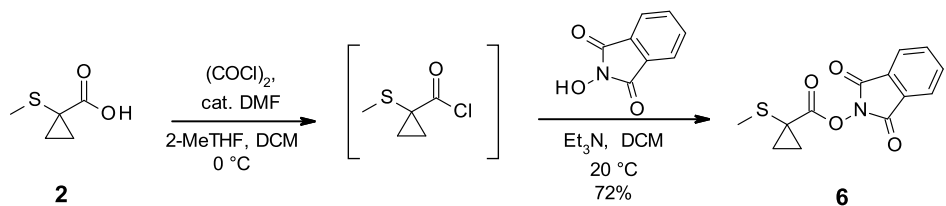
Scheme 1. Current Manufacturing Route to Ceralasertib: Minisci “Shortcut” Highlighted



Scheme 2. Promising Result Employing Classical Minisci Conditions



Scheme 3. Initial Evaluation of Sherwood's Conditions

Scheme 4. Preparation of *N*-Hydroxyphthalimide Redox Active Ester 6

With this encouraging result in hand, we carried out screening of a variety of photocatalysts in a range of solvents under batch conditions, using a 96-well plate photochemical reactor. To enable this screening work, we synthesized and isolated the *N*-hydroxyphthalimide redox active ester 6 *via* the corresponding acid chloride (Scheme 4).

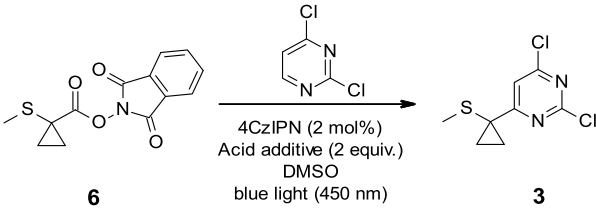
From this catalyst-screening work, we established that the catalysts 4CzIPN and [Ir(dtbbpy)(ppy)₂][PF₆]₃ resulted in the highest conversion to the desired product, and we observed DMSO to be the preferred solvent.²⁶ The organophotoredox

catalyst 4CzIPN was an attractive choice from a cost and sustainability perspective, so we decided to focus our initial reaction optimization activities on this catalyst.²⁷

The use of an acid additive in Minisci reactions is believed to be important for reactivity, as outlined by the mechanism proposed by Sherwood and co-workers.²² We therefore proceeded to evaluate a range of Brønsted and Lewis acid additives in a batch photoreactor. A variety of both Brønsted and Lewis acid additives resulted in the formation of 3, but surprisingly, we observed an inverse correlation between

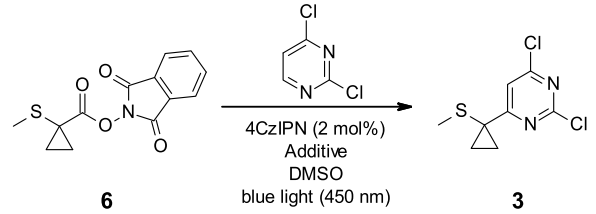
conversion to **3** (as measured by HPLC relative to an internal standard) and increasing strength of the acid additive (see Table 1).

Table 1. Effect of Acid pK_a on Conversion of **6 to **3** Using 4CzIPN**

		
acid additive	pK_a of acid (in water) ^{28,29}	product/internal standard (HPLC area counts)
trifluoroacetic acid	0.23	1.35
oxalic acid	1.23	1.35
pyruvic acid	2.39	1.61
malonic acid	2.83	1.93

Next, we conducted an experiment with triethylamine hydrochloride as an acidic additive, showing that the current Minisci reaction could proceed with a very weak acid. Remarkably, the use of the ammonium salt produced a higher solution yield using the EvoluChem photochemical reactor (Table 2). Indeed, we had doubted that the role of acid in our

Table 2. Investigation of Alternative Additives

		
entry	additive	NMR solution yield (%) ^a
1	malonic acid (2.0 equiv)	23
2	triethylamine hydrochloride (2.0 equiv)	40
3	no additive	33
4	<i>N,N</i> -diisopropylethylamine (0.2 equiv)	50

^aYields based on proton NMR of the crude reaction mixture, quantified against a known amount of an external standard (TCNB).

reaction was to protonate the heterocycle as proposed in the general mechanism of Sherwood, as our substrate, 2,4-dichloropyrimidine, is a very weak base indeed, with a calculated pK_a of -2.84 .^{22,30} We therefore performed an experiment with no acid additive present and surprisingly found that the desired product was formed in higher yield than with any of the carboxylic acid additives present. For this system, it appears that we have a combination of a particularly nucleophilic radical and an electrophilic arene, allowing for radical addition to occur in the absence of activation.

Realizing that an acid additive was not required, we decided to investigate other additives, primarily DIPEA. Interestingly, we observed an improved solution yield of 50% after 21 h using catalytic DIPEA as an additive (Table 2). The mechanistic effects of DIPEA were unknown at this point but we decided to proceed to scale-up. It was at this point in development, with reaction conditions in hand that produced

the desired product in reasonable yield, that we turned our focus to increased reaction productivity or throughput, central to this would be a move to a flow photochemistry platform.

Development of the Photoredox Minisci Reaction in Continuous Flow. The initial results in a batch photochemical reactor were encouraging, but we were acutely aware that the scale-up of photocatalytic reactions presents unique challenges.^{18,31,32} Because of the Beer–Lambert–Bouguer law, light penetration into the reaction solution is limited by the (necessarily) high molar extinction coefficient of the photocatalyst. Therefore, penetration beyond the first few millimeters of the reaction mixture is often not possible.¹⁸ For this reason, chemists have generally turned to flow reactor design to provide the required short pathlength for irradiation of the bulk of the solution, while maintaining the ability to process large quantities of the material.^{17–19,32–41}

To render the current photo-Minisci reaction viable for the manufacture of ceralasertib on a required scale of greater than 100 kg, we estimated that a minimum productivity of 5 kg/day of pyrimidine **3** would be required. Thus, although our initial focus was on reaction yield, we now focused on increasing the reaction rate to attain shorter residence times and thus higher productivity for a continuous flow process. We investigated our highest yielding batch conditions using DIPEA as an additive and 4CzIPN as a photocatalyst in DMSO using a Vapourtec UV-150 photochemical reactor with blue LEDs (450 nm). We were delighted to observe a 50% solution yield of product **3** with a residence time of 50 min which enabled complete consumption of redox active ester **6**. For comparison, the use of malonic acid as an additive required a longer residence time of 100 min to achieve complete consumption of **6** and a similar solution yield. Unfortunately, we also observed very significant darkening of the reaction mixture. We believed that this darkening would lead to diminishing returns for increases in residence time and to test this hypothesis, and to begin to improve our understanding of the reaction, we carried out some LED-NMR experiments.

LED-NMR Reaction Profiling. LED-NMR is a data-rich technique for the analysis of photocatalytic reactions *in situ*.⁴² This technique enabled us to gain detailed information on the reaction rate and profile (Figure 1), as well as highlight the formation of reaction byproducts over the course of the reaction.

Our reaction profiling confirmed the increased rate of the reaction when DIPEA (0.2 equiv) is used as an additive (Figure 1). We were able to improve yield using an excess (3 equiv) of the cheap and readily available reagent 2,4-dichloropyrimidine. However, it also became apparent that the product **3** is oxidized to sulfoxide **4** over extended time periods. Notably, oxidation to sulfoxide **4** was only observed when the redox active ester **6** was almost or fully consumed. This would be consistent with an alternative photoredox catalytic cycle becoming operative only when the redox active ester was consumed. In theory, the formation of sulfoxide **4** could be controlled by identifying the optimal flow rate, but we were interested in further improving the rate of the reaction to improve throughput.

We next carried out a series of “same-excess”-type experiments in an attempt to increase our understanding of the reaction under our best conditions using DIPEA (0.2 equiv) as an additive.⁴³ The “same-excess” experiment demonstrated that the rate of the reaction at 50% consumption of **6** is not equivalent to the rate of the reaction when the

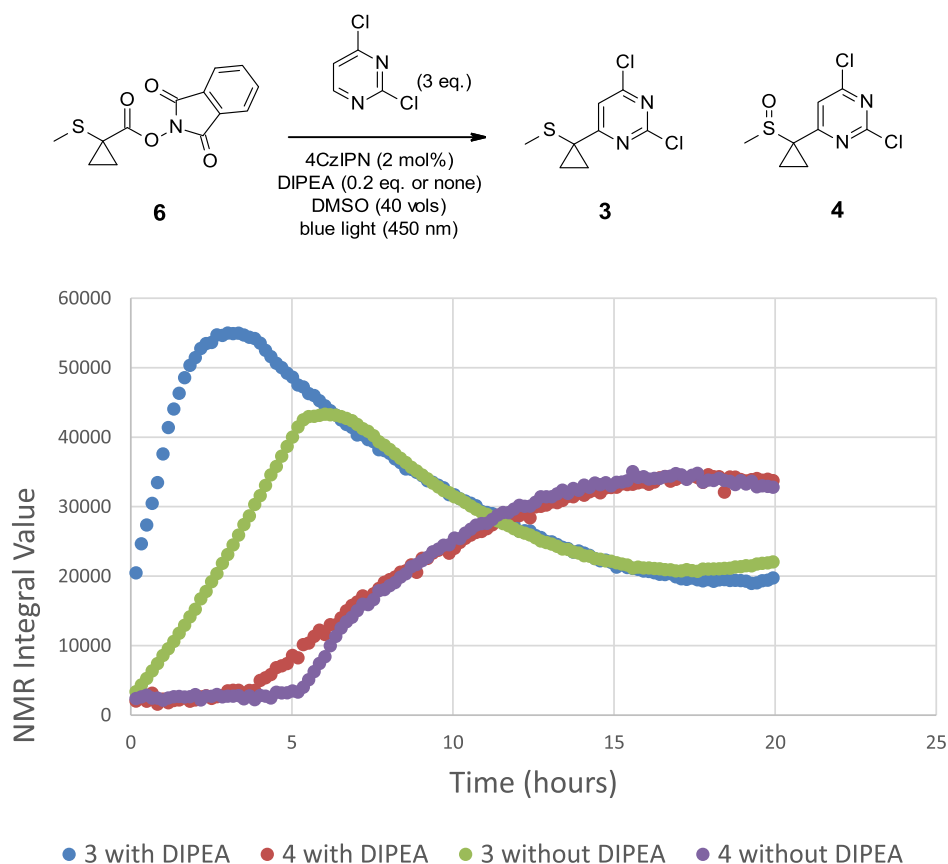


Figure 1. LED-NMR reaction profile of the 4CzIPN-catalyzed Minisci reaction with and without a DIPEA additive.

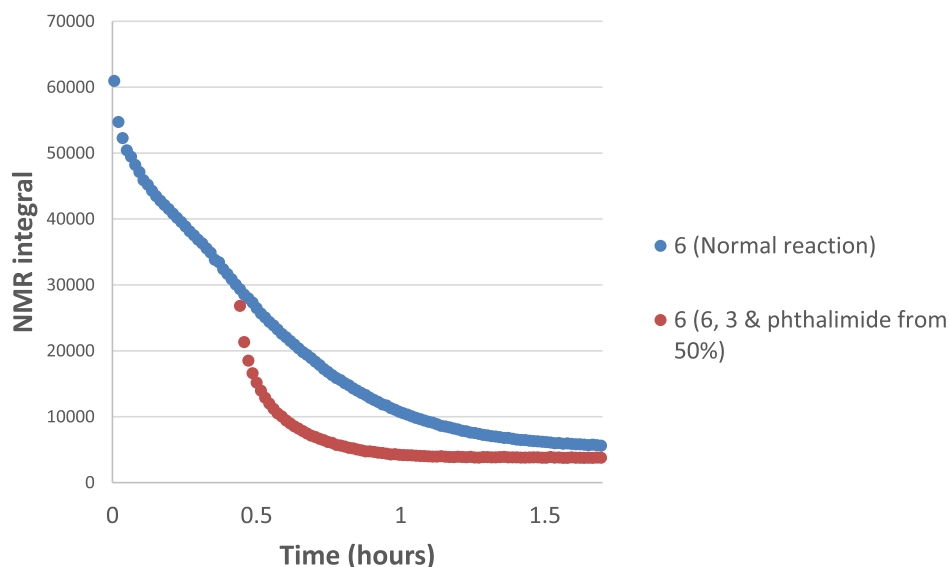


Figure 2. "Same excess" and potential product inhibition experiments.

reaction is initiated from this point, with fresh reagents at concentrations equivalent to 50% consumption of **6** (Figure 2, blue data points *vs* red data points). This would usually suggest that a product from the reaction is inhibiting the catalyst or that the catalyst is becoming "deactivated".⁴³ However, our *in situ* NMR studies had shown that the 4CzIPN catalyst was stable over the course of the reaction, so true catalyst deactivation or decomposition was not responsible for the drop in rate. Spiking experiments with the reaction product

plus phthalimide at concentrations matching those expected at 50% consumption of redox active ester **6** confirmed that the presence of product **3** or phthalimide did not inhibit the rate of the reaction (Figure 2). The key observation that the reaction mixture becomes progressively darker as the reaction progresses led us to believe that this is the cause of the reduction in the reaction rate over time. The solution darkening has the effect of reducing the number of photons that can reach the photocatalyst. Therefore, the concentration

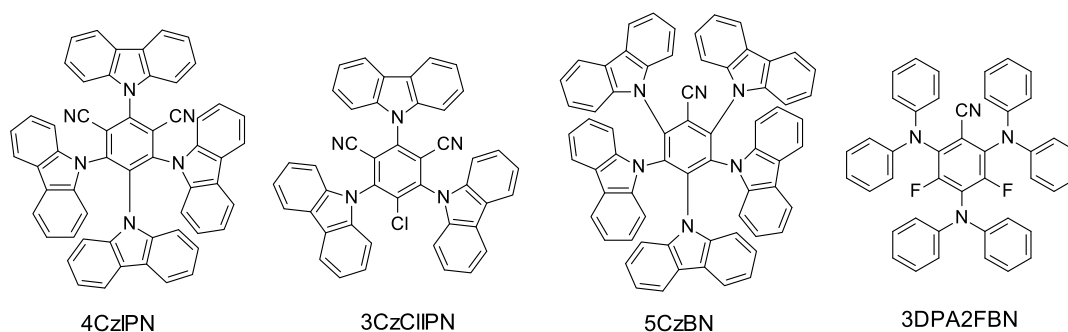


Figure 3. Structures of organophotoredox catalysts synthesized and studied.

Table 3. Comparison of Solution Yields and Redox Potentials with Different Catalyst Systems

6 **3**

photocatalyst	residence time (min) ^a	solution yield (%)	$E_{1/2}$ reduction (V vs SCE)	$E_{1/2}$ oxidation (V vs SCE)
4CzIPN	100	50	−1.18 (PC ^{•+} /PC [*])	+1.49 (PC ^{•+} /PC)
4CzIPN + DIPEA	50	55	−1.24 (PC/PC ^{•−})	+1.43 (PC [*] /PC ^{•−})
4CzIPN + DIPEA	4	26	−1.24 (PC/PC ^{•−})	+1.43 (PC [*] /PC ^{•−})
3CzCIIPN	4	7	−0.93 (PC ^{•+} /PC [*])	+1.79 (PC ^{•+} /PC)
5CzBN	13	59	−1.42 (PC ^{•+} /PC [*])	+1.41 (PC ^{•+} /PC)
5CzBN	4	29	−1.42 (PC ^{•+} /PC [*])	+1.41 (PC ^{•+} /PC)
3DPA2FBN	13	70	−1.60 (PC ^{•+} /PC [*])	+1.24 (PC ^{•+} /PC)
3DPA2FBN	4	43	−1.60 (PC ^{•+} /PC [*])	+1.24 (PC ^{•+} /PC)
3DPA2FBN + DIPEA	13	21	−1.92 (PC/PC ^{•−})	+0.92 (PC [*] /PC ^{•−})

^aResidence time is controlled by the flow rate in a 10 mL volume flow photoreactor.

of the excited photocatalyst decreases over the course of the reaction, while the total concentration of the photocatalyst (ground-state and excited-state photocatalyst) remains constant. This situation is equivalent to catalyst deactivation and results in a significant drop in the reaction rate relative to what would be expected at that stage of the reaction. With the reaction rate being our key optimization parameter, darkening of the reaction mixture over time represented a significant barrier toward carrying out this reaction on large scale.

DIPEA has the ability to quench a photoexcited catalyst, and although this appeared beneficial from a rate perspective, the resulting byproducts are likely to cause solution darkening.⁴⁴ Although we had carried out the photo-Minisci reaction with several alternative photocatalysts, a range of strongly reducing photocatalysts were absent from our screening work. The redox potential of the *N*-hydroxyphthalimide ester **6** was measured as −1.22 V *versus* SCE by cyclic voltammetry.⁴⁵ When we compare the oxidation potential of photoexcited 4CzIPN in the oxidative quenching cycle ($E_{1/2}$ PC^{•+}/PC^{*} = −1.18 V *vs* SCE) to the oxidation potential of the corresponding radical anion formed by reductive quenching of 4CzIPN with DIPEA ($E_{1/2}$ PC/PC^{•−} = −1.24 V *vs* SCE),⁴⁶ it appears that the more strongly reducing PC^{•−} from the reductive quenching cycle could have a positive impact on the rate of the reaction. We wondered if the reaction rate could be further increased by employing more reducing catalysts, also obviating the need for the addition of DIPEA. A recent study by Zeitler and co-workers showed that the redox potentials of a

class of organic photocatalysts could be effectively tuned by changing the substituents around the benzonitrile or isophthalonitrile core.⁴⁶ Using either diphenylamine or carbazole moieties as electron-donating substituents, they showed that highly reducing and highly oxidizing catalysts could be accessed. We synthesized a number of these catalysts (Figure 3, synthesis described in the Supporting Information) and carried out trial reactions with them on the photoflow reactor (Table 3).

When we compare solution yields at the shortest residence time of 4 min, it is notable that 2,4,6-tris(9*H*-carbazol-9-yl)-5-chloroisophthalonitrile (3CzCIIPN), the catalyst with the lowest reduction potential (−0.93 V *vs* SCE), gives a much lower solution yield than all other catalysts. Pleasingly, two of these catalysts showed exceptional reactivity in the current reaction, namely, 2,4,6-tris(diphenylamino)-3,5-difluorobenzonitrile (3DPA2FBN) and penta-9*H*-carbazol-9-ylbenzonitrile (5CzBN). 3DPA2FBN gave a solution yield of 70% with a 13 min residence time and 43% with a 4 min residence time. In general, more reducing photoexcited catalysts seemed to be favorable for our reaction system. However, when DIPEA was employed as an additive with 3DPA2FBN, a lower solution yield of 21% was observed, even though this system should produce a highly reducing catalyst (−1.92 V *vs* SCE). Again, significantly, more darkening of the reaction mixture was observed when DIPEA was employed as an additive, when compared to the additive-free reactions. A comparison of the 4CzIPN-DIPEA system to 3DPA2FBN was also performed by

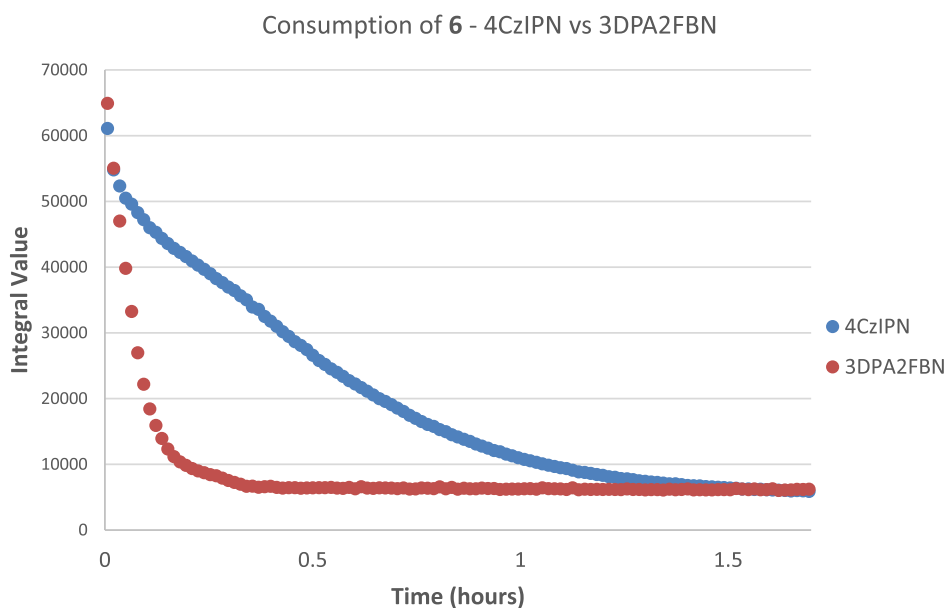


Figure 4. Comparison of 4CzIPN-DIPEA to 3DPA2FBN by LED-NMR.

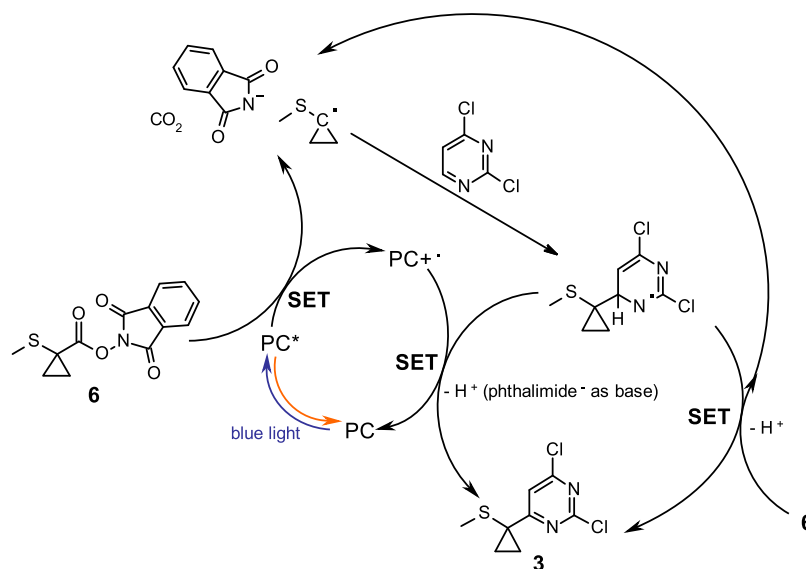


Figure 5. Proposed oxidative quenching cycle.

LED-NMR (Figure 4). Not only did we observe a significant increase in the reaction rate, we also observed no further oxidation of the desired product **3** to sulfoxide **4** when the 3DPA2FBN catalyst was used (Figure 5). The redox potential of the sulfide in product **3** was measured as +1.90 V *versus* SCE by cyclic voltammetry. The radical cation of 3DPA2FBN ($E_{1/2}$ $\text{PC}^{\bullet+}/\text{PC} = +1.24$ V *vs* SCE) is significantly less oxidizing when compared to the radical cation of 4CzIPN ($E_{1/2}$ $\text{PC}^{\bullet+}/\text{PC} = +1.49$ V *vs* SCE) and is therefore potentially unable to oxidize sulfide **3**, a plausible first step toward the formation of the sulfoxide byproduct. As stated above, we believe that some of the decrease in the rate observed for the 4CzIPN system is due to reaction darkening.

Quantum Yield Measurement and Stern–Volmer Quenching Studies. We also carried out quantum yield measurements using LED-NMR actinometry^{42,47} for both the 4CzIPN-DIPEA catalyst system and for 3DPA2FBN. The 4CzIPN-DIPEA system gave a quantum yield of 0.21, whereas

the 3DPA2FBN gave a quantum yield of 0.61. Importantly, the increased rate observed at the beginning of the reaction is maintained for most of the reaction profile for 3DPA2FBN, whereas the reaction rate tails off dramatically for the 4CzIPN-DIPEA system.

Finally, we carried out Stern–Volmer quenching studies to find out which reaction components were effective quenchers for our excited photocatalysts.^{48,49} Unsurprisingly, DIPEA quenched the 4CzIPN catalyst very effectively with a K_Q of 85 M^{-1} (Table 4), presumably forming the 4CzIPN radical anion; this is consistent with our hypothesis that the rate enhancement in moving from 4CzIPN to 4CzIPN-DIPEA is due to the formation of the more reducing and negatively charged radical anion of the photocatalyst. Also, the Stern–Volmer quenching constant for 3DPA2FBN with redox active ester **6** ($K_Q = 9.52$) is more than four times greater than that for 4CzIPN ($K_Q = 2.32$), which is consistent with a more rapid electron transfer from 3DPA2FBN. This allows an efficient redox neutral

Table 4. Stern–Volmer Quenching Studies

photocatalyst	quencher	Stern–Volmer K_Q	flow reaction solution yield (%) ^a (residence time)
4CzIPN	DIPEA	85.21	55 (50 min)
4CzIPN	6	2.32	50 (100 min)
3DPA2FBN	6	9.52	70 (13 min)
3DPA2FBN	DIPEA	3.12	21 (13 min)
5CzBN	6	12.64	59 (13 min)

^aYields based on proton NMR of the crude reaction mixture, quantified against a known amount of an external standard (TCNB).

reaction with a proposed oxidative quenching cycle (Figure 5). The final oxidation to product **3** can be achieved either *via* electron transfer to the radical cation of the photocatalyst or *via* electron transfer to another molecule of redox active ester starting material **6**, thus resulting in a radical chain process.

Development of a Suitable Work-Up. Our photoredox Minisci reaction using catalytic 3DPA2FBN was consistently giving a DMSO solution of product **3** in 65–70% yield. We believed that the yield and reaction rate could deliver a process with a suitably high throughput for large-scale manufacturing *via* continuous photoflow. However, for this reaction to be a viable manufacturing process, we needed to develop a straightforward and potentially scalable work-up. We decided to trial an aqueous work-up with an extraction into heptane. Gratifyingly, we discovered that upon addition of the reaction mixture to water (12.5 relative volumes) and heptane (25 relative volumes), >98% of the product **3** was observed in the organic layer and >99% of the phthalimide, the major reaction byproduct, resided in the aqueous layer. Also, almost all the DMSO was washed into the aqueous layer. This work-up yielded a heptane solution containing mainly **3**, some unreacted 2,4-dichloropyrimidine, and a trace of the 3DPA2FBN catalyst. Based on the hydrophilicity of 2,4-dichloropyrimidine compared to **3**, we were able to remove most of the excess 2,4-dichloropyrimidine by washing the heptane solution with a mixture of water (15 relative volumes) and DMSO (22.5 relative volumes) three times. Each sequential wash removed approximately 50% of the residual 2,4-dichloropyrimidine into the aqueous layer, with loss of only 1% of product **3** per wash. The heptane solution was then switched to a propan-2-ol solution by performing a distillative solvent swap. Finally, the product **3** was crystallized from propan-2-ol using water as an antisolvent. Although more work is required to optimize this work-up procedure for manufacturing scale, the current protocol represents a solid basis from which to develop a scalable work-up.

Results of Large-Scale Photoflow Proof of Concept.

Our optimized but not scaled up additive-free conditions using 3DPA2FBN as a catalyst worked very effectively using the Vapourtec UV-150 photochemical reactor, affording **3** in 56% isolated yield when using 3 g of redox active ester **6**. However, the throughput of material is limited by the size of the reactor. With a total reactor volume of 10 mL, a continuous flow process using our current optimized conditions at a flow rate of 0.75 mL/min would deliver approximately 32 g of product **3** over a 24 h period. We wanted to evaluate the effectiveness of our process using larger-scale continuous photoflow equipment. We were aware of the limitations of light penetration because of the Beer–Lambert–Bouguer law,^{31,32} but we were encouraged by the relative lack of solution darkening under our additive-free conditions, and we believed that we had a reasonably photon-efficient reaction, having a quantum yield of 0.61. We initially evaluated our process in a photoflow reactor with 6 mm diameter fluorinated ethylene propylene (FEP) tubing (internal diameter 4 mm), wrapped around 450 nm LEDs (100 W). The solution was preheated to 50 °C, and the pressure was controlled with a back-pressure regulator to prevent the formation of slugs of CO₂ gas (Figure 6).

Our initial evaluation using 4 mm internal diameter FEP tubing was performed using 5 equiv of 2,4-dichloropyrimidine and 2 mol % of 3DPA2FBN. A 15 mL/min flow rate, giving a residence time of 13 min, resulted in a solution yield of 24% (Table 5, entry 1). However, when the process was performed at 6 mL/min to enable 33 min residence time, we observed an encouraging solution yield of 62% (entry 2).

Using the same reagent stoichiometry but switching to FEP tubing with 8 mm internal diameter and adjusting the flow rate accordingly to give an identical residence time of 33 min resulted in a very encouraging solution yield of 65% (entry 3). A comparison of 4 and 2.5 equiv of 2,4-dichloropyrimidine charge using the 4 mm internal diameter tubing gave a slightly better yield for 4 equiv, but this benefit could be offset with a more laborious work-up to remove the excess reagent (entries 4 and 5). Maintaining the reagent stoichiometry but increasing the overall reaction concentration resulted in a lower yield (entries 6 and 7), so we decided to use 25 relative volumes of DMSO for scale-up. Finally, in an investigation of catalyst loading using the 8 mm diameter FEP tubing, a significant drop-off in yield to 38% was observed when 0.5 mol % of 3DPA2FBN was used (entry 10), but 1 mol % of catalyst was preferable to 2 mol % (entries 8 and 9). We chose to take the optimal conditions of 2,4-dichloropyrimidine (2.5 equiv), 3DPA2FBN (1 mol %), and DMSO (25 relative volumes) to scale-up using 250 g of redox active ester **6** in the 8 mm

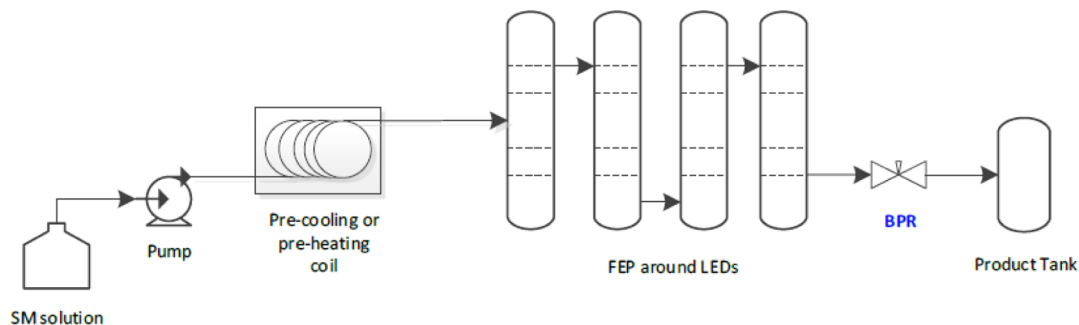
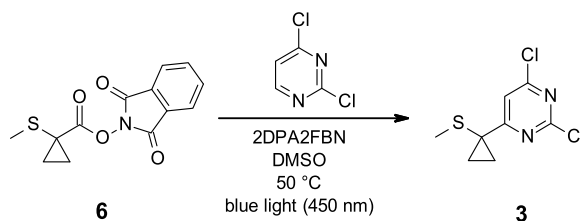


Figure 6. Schematic diagram of the large-scale photoflow reactor.

Table 5. Evaluation of the Photoredox Minisci Reaction Using Large-Scale Photoflow Equipment



entry	equiv of 2,4-dichloro-pyrimidine	catalyst loading (mol %)	DMSO volume (relative volumes)	tubing internal diameter (mm)	tubing irradiation volume (mL)	flow rate (mL/min)	residence time (min)	solution yield at steady state (%) ^a
1	5	2	25	4	200	15	13	24
2	5	2	25	4	200	6	33	62
3	5	2	25	8	100	3	33	65
4	4	2	25	4	200	6	33	61
5	2.5	2	25	4	200	6	33	54
6	4	2	12.5	4	200	6	33	48
7	2.5	2	12.5	4	200	6	33	51
8	2.5	2	25	8	100	3	33	54
9	2.5	1	25	8	100	3	33	58
10	2.5	0.5	25	8	100	3	33	38

^aYields based on proton NMR of the crude reaction mixture, quantified against a known amount of an external standard (TCNB).

internal diameter tubing (irradiated length of 2 m). The solution was pumped through the photoflow reactor at a flow rate of 3 mL/min to enable a 33 min residence time. The crude solution yield for the output solution was 52% (measured by ¹H NMR against an external standard), and this solution contained approximately 4% of the unreacted redox active ester **6**. The output solution was added to water and heptane and then the resulting heptane solution was washed with water/DMSO (2:3) to remove excess 2,4-dichloropyrimidine. Concentration of the resulting heptane solution yielded 118 g of product **3** in 44% yield (purity 79% by ¹H NMR assay). Further recrystallization of the product from propan-2-ol (236 mL) and water (24 mL) afforded **3** in 31% yield, although this crystallization process is not fully optimized.

This process is not yet fully optimized, but we were very encouraged by the yield, reaction rate, and productivity. If this process using the 8 mm internal diameter tubing was repeated on the currently available pilot-scale equipment and run continuously for 24 h, we estimate that 65 g/day of product **3** could be manufactured. However, the 8 mm diameter pilot-scale photoflow equipment has a tube length of only 2 m. We have the option to use larger-scale photoflow equipment with an internal diameter of 8 mm but with a total length of 204 m. Related photoflow equipment using UV LEDs for 2 + 2 cycloaddition was reported by Beaver and co-workers enabling a throughput of >5 kg/day.¹⁶ If we maintain the same residence time of 33 min and increase the flow rate accordingly, we can extrapolate that the productivity of the continuous flow process to generate **3** would increase to approximately 6.6 kg/day using the current conditions. Any increase in concentration or optimization of stoichiometry and yield could further improve the productivity of this process. We believe that this scalable photoredox reaction is a viable process for the future manufacture of a drug substance, and work is currently underway to further optimize this process.

CONCLUSIONS

We have carried out successful development work on an additive-free photoredox Minisci reaction. Catalyst optimiza-

tion and mechanistic understanding, resulting from LED-NMR reaction profiling and Stern–Volmer quenching studies, have enabled us to enhance significantly the rate of the reaction and avoid the phenomenon of reaction darkening. A change in catalyst also removed the unwanted over-reaction sulfoxide product. This process has been successfully scaled-up to 8 mm diameter continuous photoflow equipment, providing proof of concept on a pilot scale for this process to be used for multi-kilogram per day manufacture of the API. We believe that the current work demonstrates that visible-light photoredox catalysis has a bright future in the large-scale manufacture of pharmaceutical intermediates and API.

EXPERIMENTAL SECTION

The large-scale pilot photoflow experiments were performed using a fluorinated ethylene propylene (FEP) tubing flow cell (external diameter 10 mm, internal diameter 8 mm, wall thickness 1 mm, irradiation volume 200 mL), equipped with a back-pressure regulator. Irradiation of the FEP tubing was performed with blue LEDs (450 nm, 600 LEDs in the array, electric power 100 W, light beam geometry 90°, positioned 10 mm from FEP tubing). The light irradiation intensity was 34 mW/cm² on the surface of the reactor, and 32.5 mW/cm² was passed through the empty FEP tube. ¹H NMR spectra were recorded on a Bruker DRX 500 (500 MHz). The central peaks of dimethylsulfoxide-*d*₆ (DMSO-*d*₆; δH 2.50 ppm) was used as a reference. Spectral data are reported as a list of chemical shifts (δ, in ppm) with a description of each signal, using standard abbreviations (s = singlet, d = doublet, m = multiplet, t = triplet, q = quartet, br = broad, etc.).

Large-Scale Pilot Synthesis of 2,4-Dichloro-6-[(1,3-dioxo-1,3-dihydro-2H-indolizin-2-yl)methyl]pyrimidine (3**).** (1,3-Dioxo-1,3-dihydro-2H-indolizin-2-yl)methyl cyclopropylcarbamate (**6**, 250 g, 1.0 equiv), 2,4-dichloropyrimidine (336.12 g, 2.50 equiv), and 3DPA2FBN (5.77 g, 0.01 equiv) were dissolved in DMSO (6.25 L). The solution was sparge-degassed with nitrogen for 10 min. The resulting solution was preheated to 50 °C and pumped through a flow cell (8 mm internal

diameter, 2 m length), which was irradiated with blue visible light (450 nm) at a flow rate to enable a residence time of 33 min at steady state (back pressure 0.6–0.8 MPa). The output solution was added dropwise to a stirred mixture of water (3.12 L) and heptane (6.25 L). The layers were partitioned and then the organic layer was washed three times with a mixture of water (3.75 L) and DMSO (5.625 L). The organic layer was concentrated to yield 2,4-dichloro-6-[1-(methylsulfanyl)-cyclopropyl]pyrimidine (3, 118 g, 44% yield). Assay 79% w/w (^1H NMR).

Recrystallization of the crude product in propan-2-ol (236 mL) and water (24 mL) afforded 2,4-dichloro-6-[1-(methylsulfanyl)cyclopropyl]pyrimidine (3, 67 g, 31% yield). Assay 87% w/w (^1H NMR). ^1H NMR (500 MHz, DMSO, 27 °C) 1.42–1.55 (2H, m), 1.61–1.77 (2H, m), 2.14 (3H, s), 8.03 (1H, s); ^{13}C NMR (126 MHz, DMSO, 27 °C) 14.94, 23.02, 29.84, 117.66, 159.16, 161.92, 176.54; HRMS (ESI): calcd for $\text{C}_8\text{H}_9\text{N}_2\text{SCl}_2$ $[\text{M} + \text{H}]^+$, 234.9858; found, 234.9863.

■ ASSOCIATED CONTENT

■ Supporting Information

The Supporting Information is available free of charge at <https://pubs.acs.org/doi/10.1021/acs.oprd.0c00483>.

Details of screening experiments, batch photochemistry, small-scale photoflow, ^1H NMR spectra, Stern–Volmer quenching studies, and quantum yield measurement and cyclic voltammetry (PDF)

■ AUTHOR INFORMATION

Corresponding Authors

Mark A. Graham – Chemical Development, Pharmaceutical Technology & Development, Operations, AstraZeneca, Macclesfield SK10 2NA, U.K.; orcid.org/0000-0001-7186-9107; Email: mark.a.graham@astrazeneca.com

Gary Noonan – Chemical Development, Pharmaceutical Technology & Development, Operations, AstraZeneca, Macclesfield SK10 2NA, U.K.; Email: Gary.Noonan1@astrazeneca.com

Authors

Janette H. Cherryman – Chemical Development, Pharmaceutical Technology & Development, Operations, AstraZeneca, Macclesfield SK10 2NA, U.K.

James J. Douglas – Early Chemical Development, Pharmaceutical Sciences, R&D, AstraZeneca, Macclesfield SK10 2NA, U.K.; orcid.org/0000-0002-9681-0459

Miguel Gonzalez – Asymchem Laboratories (Tianjin) Co. Ltd., TEDA, Tianjin 300457, P. R. China

Lucinda V. Jackson – Chemical Development, Pharmaceutical Technology & Development, Operations, AstraZeneca, Macclesfield SK10 2NA, U.K.

Kevin Leslie – Chemical Development, Pharmaceutical Technology & Development, Operations, AstraZeneca, Macclesfield SK10 2NA, U.K.

Zhi-qing Liu – Asymchem Laboratories (Tianjin) Co. Ltd., TEDA, Tianjin 300457, P. R. China

David McKinney – Chemical Development, Pharmaceutical Technology & Development, Operations, AstraZeneca, Macclesfield SK10 2NA, U.K.

Rachel H. Munday – Chemical Development, Pharmaceutical Technology & Development, Operations, AstraZeneca, Macclesfield SK10 2NA, U.K.

Chris D. Parsons – Early Chemical Development, Pharmaceutical Sciences, R&D, AstraZeneca, Macclesfield SK10 2NA, U.K.

David T. E. Whittaker – Early Chemical Development, Pharmaceutical Sciences, R&D, AstraZeneca, Macclesfield SK10 2NA, U.K.

En-xuan Zhang – Asymchem Laboratories (Tianjin) Co. Ltd., TEDA, Tianjin 300457, P. R. China

Jun-wang Zhang – Asymchem Laboratories (Tianjin) Co. Ltd., TEDA, Tianjin 300457, P. R. China

Complete contact information is available at: <https://pubs.acs.org/doi/10.1021/acs.oprd.0c00483>

■ Author Contributions

The manuscript was written by M.A.G. and G.N. through contributions of all authors. All authors have given approval to the final version of the manuscript.

■ Notes

The authors declare no competing financial interest.

■ ACKNOWLEDGMENTS

The authors would like to thank Gair Ford, Peter Hamilton, Martin Jones, Rita Galan, Adam Clarke, Carl Mallia, Niall McCreanor, Anne O’Kearney McMullan, Simone Tomasi, Robert Cox, and Ian Ashworth for helpful discussions. The authors would like to thank Emma Randles and Andrew Ray for analytical support.

■ ABBREVIATIONS

API, active pharmaceutical ingredient; CSA, camphorsulfonic acid; 5CzBN, penta-9H-carbazol-9-ylbenzonitrile; 3CzClIPN, 2,4,6-tri(9H-carbazol-9-yl)-5-chloroisophthalonitrile; 4CzIPN, 1,2,3,5-tetrakis(carbazol-9-yl)-4,6-dicyanobenzene; DCM, dichloromethane; DIC, diisopropylcarbodiimide; DIPEA, *N,N*-diisopropylethylamine; DMAP, *N,N*-dimethylaminopyridine; DMF, *N,N*-dimethylformamide; 3DPA2FBN, 2,4,6-tris-(diphenylamino)-3,5-difluorobenzonitrile; LED, light-emitting diode; MS, mass spectrum; NMR, nuclear magnetic resonance; PC, photocatalyst; SCE, saturated calomel electrode; SET, single electron transfer; V, volt

■ REFERENCES

- (1) Foote, K. M.; Nissink, J. W. M.; McGuire, T.; Turner, P.; Guichard, S.; Yates, J. W. T.; Lau, A.; Blades, K.; Heathcote, D.; Odedra, R.; Wilkinson, G.; Wilson, Z.; Wood, C. M.; Jewsbury, P. J. Discovery and Characterization of AZD6738, a Potent Inhibitor of Ataxia Telangiectasia Mutated and Rad3 Related (ATR) Kinase with Application as an Anticancer Agent. *J. Med. Chem.* **2018**, *61*, 9889–9907.
- (2) Foote, K. M.; Nissink, J. W. M.; Turner, P. Morpholino pyrimidines and their use in therapy. WO 2011154737 A1, 2011.
- (3) Goundry, W. R. F.; Dai, K.; Gonzalez, M.; Legg, D.; O’Kearney-McMullan, A.; Morrison, J.; Stark, A.; Siedlecki, P.; Tomlin, P.; Yang, J. Development and Scale-up of a Route to ATR Inhibitor AZD6738. *Org. Process Res. Dev.* **2019**, *23*, 1333–1342.
- (4) Henssen, A. G.; Reed, C.; Jiang, E.; Garcia, H. D.; von Stebut, J.; MacArthur, I. C.; Hundsdoerfer, P.; Kim, J. H.; de Stanchina, E.; Kuwahara, Y.; Hosoi, H.; Ganem, N. J.; Dela Cruz, F.; Kung, A. L.; Schulte, J. H.; Petrini, J. H.; Kentsis, A. Therapeutic targeting of PGBD5-induced DNA repair dependency in pediatric solid tumors. *Sci. Transl. Med.* **2017**, *9*, 9078.
- (5) Graham, M. A.; Askey, H.; Campbell, A. D.; Chan, L.; Cooper, K. D.; Cui, Z.; Dalgleish, A.; Dave, D.; Ensor, G.; Galan, R.; Hamilton, P.; Heffernan, C.; Jackson, L. V.; Jones, M. F.; Mulholland, K. R.

- Pervez, M.; Popadyne, M.; Randles, E.; Tomasi, S.; Wang, S. Development and Scale-up of an Improved Manufacturing Route to the ATR Inhibitor Ceralasertib. *Org. Process Res. Dev.* **2020**, DOI: 10.1021/acs.oprd.0c00482.
- (6) Graham, M. A.; Jackson, L. V.; Noonan, G. M.; Inglesby, P. A.; Dave, D. P.; Cooper, K. G. Pharmaceutical process and intermediates. WO 2020127208 A2, 2020.
- (7) Minisci, F.; Bernardi, R.; Bertini, F.; Galli, R.; Perchinummo, M. Nucleophilic character of alkyl radicals—VI. *Tetrahedron* **1971**, 27, 3575–3579.
- (8) Proctor, R. S. J.; Phipps, R. J. Recent Advances in Minisci-Type Reactions. *Angew. Chem., Int. Ed. Engl.* **2019**, 58, 13666–13699.
- (9) Mai, W.-P.; Sun, B.; You, L.-Q.; Yang, L.-R.; Mao, P.; Yuan, J.-W.; Xiao, Y.-M.; Qu, L.-B. Silver catalysed decarboxylative alkylation and acylation of pyrimidines in aqueous media. *Org. Biomol. Chem.* **2015**, 13, 2750–2755.
- (10) Shore, D. G. M.; Wasik, K. A.; Lyssikatos, J. P.; Estrada, A. A. Minisci alkylations of electron-deficient pyrimidines with alkyl carboxylic acids. *Tetrahedron Lett.* **2015**, 56, 4063–4066.
- (11) Marzo, L.; Pagire, S. K.; Reiser, O.; König, B. Visible-Light Photocatalysis: Does It Make a Difference in Organic Synthesis? *Angew. Chem., Int. Ed. Engl.* **2018**, 57, 10034–10072.
- (12) Douglas, J. J.; Sevrin, M. J.; Stephenson, C. R. J. Visible Light Photocatalysis: Applications and New Disconnections in the Synthesis of Pharmaceutical Agents. *Org. Process Res. Dev.* **2016**, 20, 1134–1147.
- (13) Prier, C. K.; Rankic, D. A.; MacMillan, D. W. C. Visible Light Photoredox Catalysis with Transition Metal Complexes: Applications in Organic Synthesis. *Chem. Rev.* **2013**, 113, 5322–5363.
- (14) Romero, N. A.; Nicewicz, D. A. Organic Photoredox Catalysis. *Chem. Rev.* **2016**, 116, 10075–10166.
- (15) McAtee, R. C.; McClain, E. J.; Stephenson, C. R. J. Illuminating Photoredox Catalysis. *Trends Chem.* **2019**, 1, 111–125.
- (16) Beaver, M. G.; Zhang, E.-x.; Liu, Z.-q.; Zheng, S.-y.; Wang, B.; Lu, J.-p.; Tao, J.; Gonzalez, M.; Jones, S.; Tedrow, J. S. Development and Execution of a Production-Scale Continuous [2 + 2] Photocycloaddition. *Org. Process Res. Dev.* **2020**, 24, 2139–2146.
- (17) Harper, K. C.; Moschetta, E. G.; Bordawekar, S. V.; Wittenberger, S. J. A Laser Driven Flow Chemistry Platform for Scaling Photochemical Reactions with Visible Light. *ACS Cent. Sci.* **2019**, 5, 109–115.
- (18) Noel, T. *Photochemical Processes in Continuous-Flow Reactors: From Engineering Principles to Chemical Applications*, 1st ed.; World Scientific Publishing Europe Ltd, 2017; p 271.
- (19) Corcoran, E. B.; McMullen, J. P.; Lévesque, F.; Wismer, M. K.; Naber, J. R.; McMullen, J. P.; Levesque, F.; Wismer, M. K.; Naber, J. R. Photon Equivalents as a Parameter for Scaling Photoredox Reactions in Flow: Translation of Photocatalytic C–N Cross-Coupling from Lab Scale to Multikilogram Scale. *Angew. Chem., Int. Ed. Engl.* **2020**, 59, 11964–11968.
- (20) Grimm, I.; Hauer, S. T.; Schulte, T.; Wycich, G.; Collins, K. D.; Lovis, K.; Candish, L. Upscaling Photoredox Cross-Coupling Reactions in Batch Using Immersion-Well Reactors. *Org. Process Res. Dev.* **2020**, 24, 1185–1193.
- (21) Cheng, W.-M.; Shang, R.; Fu, M.-C.; Fu, Y. Photoredox-Catalysed Decarboxylative Alkylation of N-Heteroarenes with N-(Acyloxy)phthalimides. *Chemistry* **2017**, 23, 2537–2541.
- (22) Sherwood, T. C.; Li, N.; Yazdani, A. N.; Dhar, T. G. M. Organocatalyzed, Visible-Light Photoredox-Mediated, One-Pot Minisci Reaction Using Carboxylic Acids via N-(Acyloxy)phthalimides. *J. Org. Chem.* **2018**, 83, 3000–3012.
- (23) Sherwood, T. C.; Xiao, H.-Y.; Bhaskar, R. G.; Simmons, E. M.; Zaretsky, S.; Rauch, M. P.; Knowles, R. R.; Dhar, T. G. M. Decarboxylative Intramolecular Arene Alkylation Using N-(Acyloxy)-phthalimides, an Organic Photocatalyst, and Visible Light. *J. Org. Chem.* **2019**, 84, 8360–8379.
- (24) Kammer, L. M.; Rahman, A.; Opatz, T. A Visible Light-Driven Minisci-Type Reaction with N-Hydroxyphthalimide Esters. *Molecules* **2018**, 23, 764.
- (25) Details of by-products in [Supporting Information](#).
- (26) See [Supporting Information](#) for further details.
- (27) Shang, T.-Y.; Lu, L.-H.; Cao, Z.; Liu, Y.; He, W.-M.; Yu, B. Recent advances of 1,2,3,5-tetrakis(carbazol-9-yl)-4,6-dicyanobenzene (4CzIPN) in photocatalytic transformations. *Chem. Commun.* **2019**, 55, 5408–5419.
- (28) Dippy, J. F. J.; Hughes, S. R. C.; Rozanski, A. 498. The dissociation constants of some symmetrically disubstituted succinic acids. *J. Chem. Soc.* **1959**, 2492.
- (29) Braude, E. A.; Nachod, F. C. *Determination of Organic Structures by Physical Methods*; Academic Press: New York, 1955.
- (30) Calculated using Advanced Chemistry Development (ACD/Labs) Software V11.02 (1994–2020 ACD/Labs).
- (31) Moschetta, E. G.; Richter, S. M.; Wittenberger, S. J. Heuristics, Protocol, and Considerations for Flow Chemistry in Photoredox Catalysis. *ChemPhotoChem* **2017**, 1, 539–543.
- (32) Bonfield, H. E.; Knauber, T.; Levesque, F.; Moschetta, E. G.; Susanne, F.; Edwards, L. J. Photons as a 21st century reagent. *Nat. Commun.* **2020**, 11, 804.
- (33) Cambié, D.; Bottecchia, C.; Straathof, N. J. W.; Hessel, V.; Noël, T. Applications of Continuous-Flow Photochemistry in Organic Synthesis, Material Science, and Water Treatment. *Chem. Rev.* **2016**, 116, 10276–10341.
- (34) Politano, F.; Oksdath-Mansilla, G. Light on the Horizon: Current Research and Future Perspectives in Flow Photochemistry. *Org. Process Res. Dev.* **2018**, 22, 1045–1062.
- (35) VanHeyst, M. D.; Qi, J.; Roecker, A. J.; Hughes, J. M. E.; Cheng, L.; Zhao, Z.; Yin, J. Continuous Flow-Enabled Synthesis of Bench-Stable Bicyclo[1.1.1]pentane Trifluoroborate Salts and Their Utilization in Metallaphotoredox Cross-Couplings. *Org. Lett.* **2020**, 22, 1648–1654.
- (36) Halperin, S. D.; Kwon, D.; Holmes, M.; Regalado, E. L.; Campeau, L.-C.; DiRocco, D. A.; Britton, R. Development of a Direct Photocatalytic C–H Fluorination for the Preparative Synthesis of Odanacatib. *Org. Lett.* **2015**, 17, 5200–5203.
- (37) Reiser, O. Blue Chemistry: Trifluoromethylations Going Large! *Chem* **2016**, 1, 344–345.
- (38) Beatty, J. W.; Douglas, J. J.; Miller, R.; McAtee, R. C.; Cole, K. P.; Stephenson, C. R. J. Photochemical Perfluoroalkylation with Pyridine N-Oxides: Mechanistic Insights and Performance on a Kilogram Scale. *Chem* **2016**, 1, 456–472.
- (39) Yayla, H. G.; Peng, F.; Mangion, I. K.; McLaughlin, M.; Campeau, L.-C.; Davies, I. W.; DiRocco, D. A.; Knowles, R. R. Discovery and mechanistic study of a photocatalytic indoline dehydrogenation for the synthesis of elbasvir. *Chem. Sci.* **2016**, 7, 2066–2073.
- (40) Bonfield, H. E.; Mercer, K.; Diaz-Rodriguez, A.; Cook, G. C.; McKay, B. S. J.; Slade, P.; Taylor, G. M.; Ooi, W. X.; Williams, J. D.; Roberts, J. P. M.; Murphy, J. A.; Schermund, L.; Kroutil, W.; Mielke, T.; Cartwright, J.; Grogan, G.; Edwards, L. J. The Right Light: De Novo Design of a Robust Modular Photochemical Reactor for Optimum Batch and Flow Chemistry. *ChemPhotoChem* **2019**, 4, 45–51.
- (41) Steiner, A.; Roth, P. M. C.; Strauss, F. J.; Gauron, G.; Tekautz, G.; Winter, M.; Williams, J. D.; Kappe, C. O. Multikilogram per Hour Continuous Photochemical Benzylic Brominations Applying a Smart Dimensioning Scale-up Strategy. *Org. Process Res. Dev.* **2020**, 24, 2208–2216.
- (42) Ji, Y.; DiRocco, D. A.; Kind, J.; Thiele, C. M.; Gschwind, R. M.; Reibarkh, M. LED-Illuminated NMR Spectroscopy: A Practical Tool for Mechanistic Studies of Photochemical Reactions. *ChemPhotoChem* **2019**, 3, 984–992.
- (43) Blackmond, D. G. Kinetic Profiling of Catalytic Organic Reactions as a Mechanistic Tool. *J. Am. Chem. Soc.* **2015**, 137, 10852–10866.
- (44) Beatty, J. W.; Stephenson, C. R. J. Amine Functionalization via Oxidative Photoredox Catalysis: Methodology Development and Complex Molecule Synthesis. *Acc. Chem. Res.* **2015**, 48, 1474–1484.
- (45) Details in [Supporting Information](#).

(46) Speckmeier, E.; Fischer, T. G.; Zeitler, K. A Toolbox Approach To Construct Broadly Applicable Metal-Free Catalysts for Photo-redox Chemistry: Deliberate Tuning of Redox Potentials and Importance of Halogens in Donor–Acceptor Cyanoarenes. *J. Am. Chem. Soc.* **2018**, *140*, 15353–15365.

(47) Ji, Y.; DiRocco, D. A.; Hong, C. M.; Wismer, M. K.; Reibarkh, M. Facile Quantum Yield Determination via NMR Actinometry. *Org. Lett.* **2018**, *20*, 2156–2159.

(48) Pitre, S. P.; McTiernan, C. D.; Scaiano, J. C. Understanding the Kinetics and Spectroscopy of Photoredox Catalysis and Transition-Metal-Free Alternatives. *Acc. Chem. Res.* **2016**, *49*, 1320–1330.

(49) Buzzetti, L.; Crisenza, G. E. M.; Melchiorre, P. Mechanistic Studies in Photocatalysis. *Angew. Chem., Int. Ed. Engl.* **2019**, *58*, 3730–3747.